

Received 8 December 2023; revised 10 February 2024 and 16 March 2024; accepted 10 April 2024. Date of publication 26 April 2024;
date of current version 9 May 2024. The review of this article was arranged by Editor Paolo Bonato.

Digital Object Identifier 10.1109/OJEMB.2024.3391939

Pulsed Low-Intensity Focused Ultrasound (LIFU) Activation of Ovarian Follicles

YAN XIAO ^{ID}^{1,2}, LIXIA YANG ^{ID}³, YICONG WANG ^{ID}^{1,2}, YU WANG ^{ID}^{1,2}, YUNING CHEN ^{ID}¹, WENHAN LU ^{ID}⁴,
ZHENLE PEI ^{ID}¹, RUONAN ZHANG ^{ID}¹, YAO YE ^{ID}⁵, XIAOWEI JI ^{ID}⁵, SUYING LIU ^{ID}⁵, XI DONG ^{ID}⁵,
YONGHUA XU ^{ID}³, AND YI FENG ^{ID}^{1,2}

¹Department of Integrative Medicine and Neurobiology, School of Basic Medical Sciences, Shanghai Medical College, Brain Science Collaborative Innovation Center, State Key Laboratory of Medical Neurobiology, Fudan University, Shanghai 200032, China

²Shanghai Key Laboratory of Acupuncture Mechanism and Acupoint Function, Shanghai Institute of Acupuncture and Moxibustion, Shanghai 200433, China

³Department of Imaging and Interventional Radiology, Zhongshan-Xuhui Hospital of Fudan University/Xuhui Center Hospital, Shanghai 200031, China

⁴Department of Ophthalmology & Visual Science, Eye & ENT Hospital, Shanghai Medical College, Fudan University, Shanghai 200031, China

⁵Reproductive Medicine Center, Zhongshan Hospital, Fudan University, Shanghai 200032, China

CORRESPONDING AUTHORS: YONGHUA XU; YI FENG (e-mail: howardyonghua@yeah.net, fengyi17@fudan.edu.cn)

This work was supported in part by The National Natural Science Foundation of China provided support for this study, NSFC under Grant 81973945 and Grant 82174497 issued to Yi Feng, and in part by the Innovative Research Team of High-Level Local Universities in Shanghai. The work of Yi Feng was supported by the Development Project of Shanghai Peak Disciplines-Integrated Chinese and Western Medicine, under Grant 20180101.

Yan Xiao and Lixia Yang contributed equally to this work.

This article has supplementary downloadable material available at <https://doi.org/10.1109/OJEMB.2024.3391939>, provided by the authors.

ABSTRACT *Objective:* A biological system's internal morphological structure or function can be changed as a result of the mechanical effect of focused ultrasound. Pulsed low-intensity focused ultrasound (LIFU) has mechanical effects that might induce follicle development with less damage to ovarian tissue. The potential development of LIFU as a non-invasive method for the treatment of female infertility is being considered, and this study sought to explore and confirm that LIFU can activate ovarian follicles. *Results:* We found a 50% increase in ovarian weight and in the number of mature follicles on the ultrasound-stimulated side with pulsed LIFU and intraperitoneal injection of 10 IU PMSG in 10-day-old rats. After ultrasound stimulation, the PCOS-like rats had a decrease in androgen levels, restoration of regular estrous cycle and increase in the number of mature follicles and corpora lutea, and the ratio of M1 and M2 type macrophages was altered in antral follicles of PCOS-like rats, consequently promoting further development and maturation of antral follicles. *Conclusion:* LIFU treatment could trigger actin changes in ovarian cells, which might disrupt the Hippo signal pathway to promote follicle formation, and the mechanical impact on the ovaries of PCOS-like rats improved antral follicle development.

INDEX TERMS Focused ultrasound, follicle development, polycystic ovary syndrome.

IMPACT STATEMENT LIFU promotes ovarian follicle development.

I. INTRODUCTION

Premature ovarian insufficiency (POI) and polycystic ovary syndrome (PCOS) are widely recognized as the primary etiological factors contributing to female infertility. A meta-analysis estimated that 3.7% of women worldwide suffer from POI [1]. According to some reports, the incidence of PCOS may vary between 10 to 20% [2], [3]. Studies have shown that surgical mechanical stimulation of POI ovaries can activate dormant follicle development [4], [5], but this technique

is invasive and can lead to complications [6]. As a result, extensive research has been conducted in the realm of reproductive medicine pertaining to the stimulation of inactive follicles in the ovaries of individuals diagnosed with POI and the stimulation of antral follicles in the ovaries of individuals diagnosed with PCOS.

Ultrasound has become an essential tool for both diagnostic and therapeutic purposes in modern medical applications [7]. The mechanical, thermal, and cavitation effects are the three

primary impacts that focused ultrasound can have. Over the course of several decades, HIFU has been widely employed in the therapeutic setting for the purpose of tumor ablation [8], [9], [10], [11] and has accumulated more than 100000 cases of successful ablation of uterine fibroids and endometriosis [12], and post-treatment follow-up has shown that it can improve patients' conception rates [13], [14]. However, the application of HIFU can induce mechanical effects that lead to the deformation or potential fracture of the microstructure of biological tissues due to stress. Therefore, we hypothesized that the mechanical stress of focused ultrasound promotes follicular development. In a review of previous studies, Abtahi et al. found that therapeutic ultrasound accelerated and increased revascularization and helped promote ovarian follicle growth [15]. In addition, low-intensity pulsed ultrasound (LIPUS)therapy can enhance angiogenesis by promoting YAP nuclear translocation through the Hippo signaling pathway [16]. Tang et al. reported that LIPUS can rescue cyclophosphamide-induced POI in rats [17]. The researchers' investigation revealed that the use of ultrasound therapy resulted in a decrease in the number of atretic follicles attributed to POI, while concurrently elevating estrogen levels. These findings indicate that LIFU may at least partially restore ovarian functionality in individuals diagnosed with POI [17]. Other studies have proposed focused ultrasound as a potential treatment for PCOS [18], [19], and another found that LIPUS demonstrated a mitigating effect on the apoptotic and inflammatory conditions associated with ovarian injury generated by 4-vinyl cyclohexene diepoxide. This intervention resulted in concomitant alterations in cellular structures [20]. Building on the above research, we performed pulsed LIFU treatment directly on ovaries to mitigate the potential harm inflicted upon ovarian tissues due to the thermal effects of HIFU.

II. RESULTS

A. LIFU PROMOTES FOLLICULAR DEVELOPMENT IN 10-DAY-OLD RATS

In this study, LIFU was used to induce stimulation in the ovaries of 10-day-old rats (Fig. 1(a)). A total of 10 IU PMSG was injected at the end of surgery in the untreated ovary, and the rats were sacrificed 5 days later (Fig. 1(b)). We found that 2 W LIFU had the potential to increase the weight of the ovaries. On the other hand, 8 W LIFU caused damage to the tissues and to a considerable decrease in the weight of the ovaries (Fig. 1(c)). In addition, we found that there was a tendency to increase the weight of the ovary on the LIFU-stimulated side at 3–4 days, and the increase in the weight of the ovary was more pronounced at day 5 (Fig. 1(c)). H&E staining revealed mature follicles on the LIFU-stimulated side (Fig. 1(e)). To further explore the changes in the internal structure of the ovary, follicles were counted at different developmental stages in the intact ovary by the iDISCO hyalinization method (Fig. 1(f)–(g)). We observed more mature follicles on the side that was activated with ultrasound than on the control side (Fig. 1(h)).

B. MACROPHAGES AND YAP ARE INVOLVED IN LIFU-INDUCED FOLLICULAR DEVELOPMENT

Given that macrophages are the main type of immune cell in ovarian tissues and are very important for keeping those tissues in balance, it is imperative to investigate their functionality in relation to the etiology of PCOS. The iDISCO method was used to observe the number of macrophages in different follicle stages throughout the ovary and showed that the number of macrophages tended to increase as the follicles matured (Fig. 2(a) and (b)). These effects have been observed to have the capacity to stimulate an immunological response, specifically the activation of macrophages[21], [22], [23]. Consequently, alterations in the macrophage population inside ovarian tissue were identified after LIFU stimulation, and we observed increased numbers of macrophages (Fig. 2(c) and (d)). In addition, YAP, an important part of the Hippo signaling system, plays a significant role in the regulation of organ growth and development[24], and studies have shown that mechanical stimulation can trigger YAP expression [25], [26], [27]. Therefore, we wanted to verify whether the acoustic radiation of focused LIFU acts on YAP and whether the increase in ovarian weight we observed after ultrasound stimulation was related to changes in macrophage numbers and to the entry of YAP into the nucleus. We performed co-localization analysis of macrophages and YAP and found that the increase in macrophages after LIFU stimulation could simultaneously increase the expression of YAP in granulocytes (Fig. 2(e)).

C. LIFU PROMOTES FOLLICULAR DEVELOPMENT IN THE OVARY THROUGH THE HIPPO SIGNALING SYSTEM

The Hippo pathway is crucial in the regulation of organ growth [25], [27], [26], [28]. In the current investigation, it was observed that there was an increase in nuclear YAP expression (Fig. 3(a) and (b)) and a decline in cytoplasmic P-YAP expression (Fig. 3(c) and (d)) in ovarian tissues following 3-hour stimulation with LIFU. These findings indicate that the mechanical impact of focused ultrasound impeded the Hippo signaling pathway, resulting in enhanced YAP translocation into the nucleus. The expression of the *CCN* family and *BIRC* family of molecules downstream of YAP were examined (Fig. 3(e)), and we found that CCN1 and CCN2 increased after 6 h of LIFU stimulation (Fig. 3(f)–(h)). Furthermore, immunofluorescence was used to examine the nuclear translocation of YAP at 1 hour and 3 hours following LIFU treatment (S. 1a). It was observed that the co-localization signals of YAP and DAPI increased at the 3-hour time point after LIFU treatment (S. 1b). Consequently, this resulted in increased synthesis of CCN1 and CCN2, thus stimulating follicular development.

D. LIFU IMPROVES HORMONE LEVELS AND OVARIAN FUNCTION IN PCOS-LIKE RATS

The PCOS model was created as shown in Fig. 4(a). At the end of modeling, the rats were subjected to bilateral focused

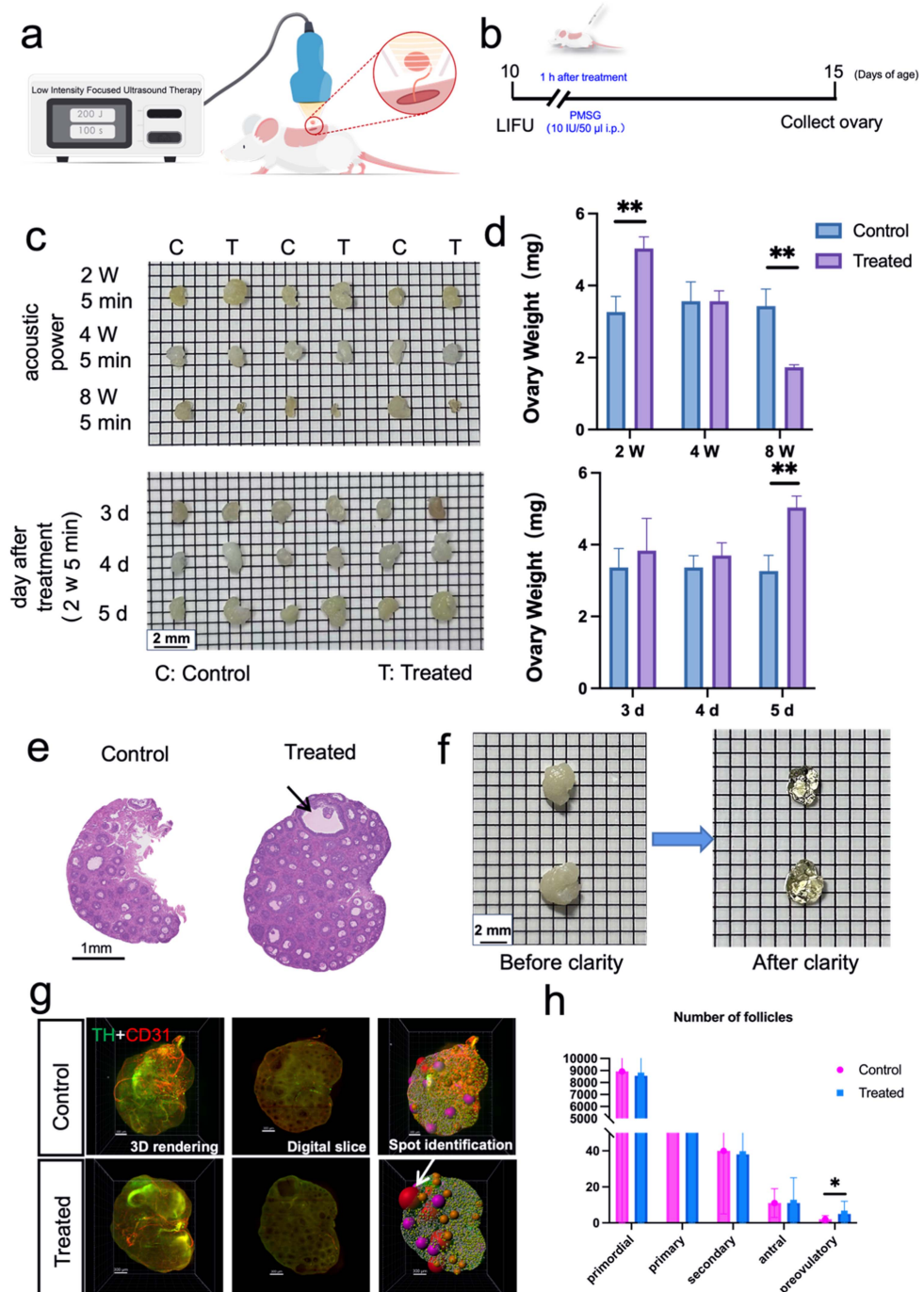


FIGURE 1. LIFU treatments, the comparison of treated and control ovary size, and the comparison of the differences between treatments at different power levels. (a) Diagram of the treatment modalities. (b) PMSG injection after 1 h of LIFU treatment and removal of ovaries after 5 days. (c) Changes in ovary weight at different ultrasound power levels and at different sampling time points. (d) Weight change per group. (e) H&E staining of the treatment and control groups. (f) Ovaries before and after clearing. (g) Counts of ovarian follicles using the *spots* function in Imaris. (h) Number of follicles at each developmental stage. Results are presented as means \pm SEM. *p < 0.05, **p < 0.01 vs. Control group (n = 6).

ultrasound stimulation of the ovaries, and ovarian tissue and serum were collected from the rats two weeks following treatment. The ovarian weight of rats with PCOS was found to decrease after receiving LIFU treatment (Fig. 4(c)). Staining with H&E revealed a greater number of antral follicles in the model group and neoplastic follicles following LIFU

treatment (Fig. 4(b)). In accordance with existing research, it was observed that the model group exhibited elevated serum testosterone levels and greater ratios of luteinizing hormone to follicle-stimulating hormone compared to the control group, and this abnormality was ameliorated by LIFU treatment (Fig. 4(d)). Irregular motility cycles in the model group could

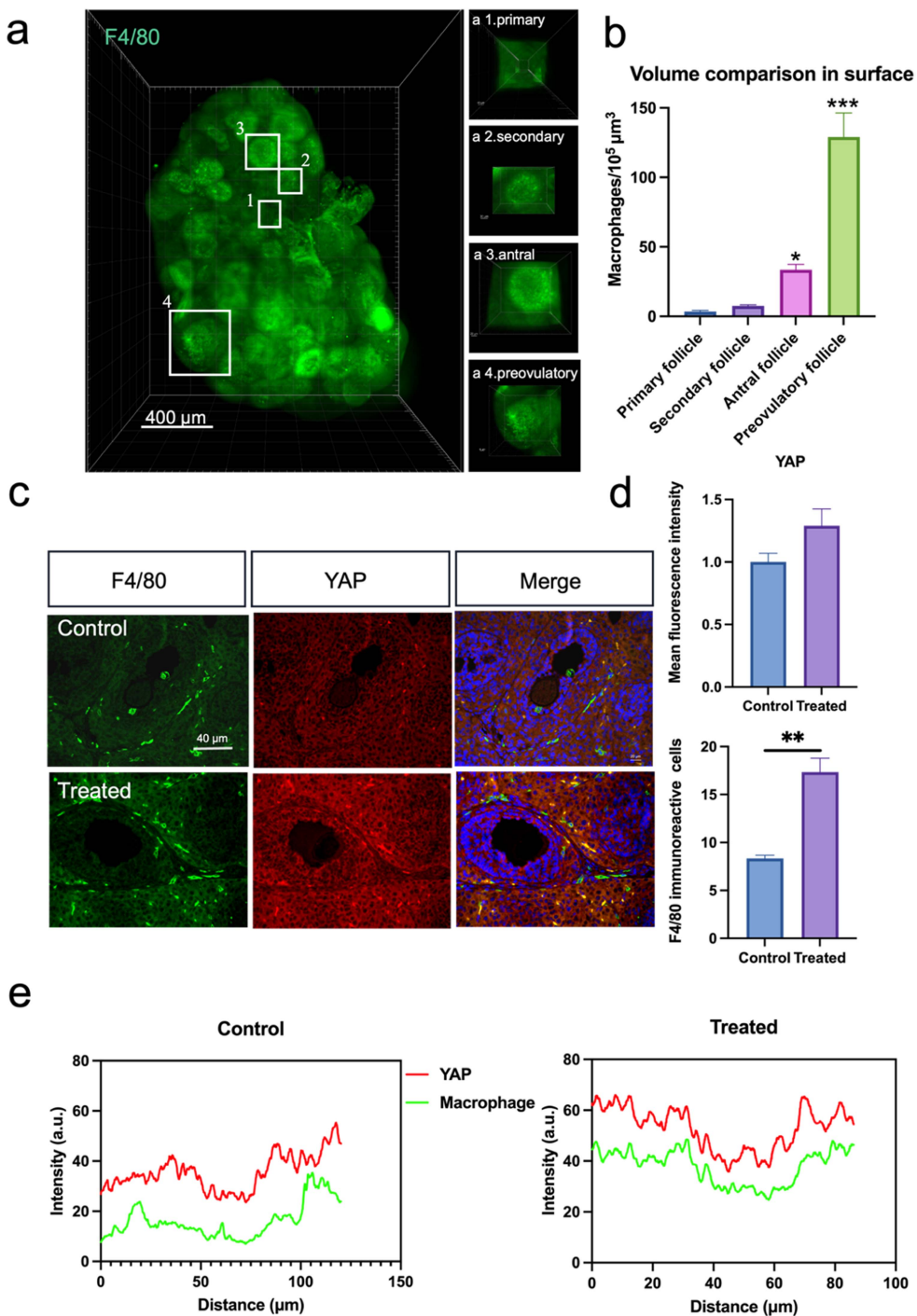


FIGURE 2. Involvement of macrophages and YAP in follicular growth and development. (a) The follicular macrophage volume increased as follicles matured. (b) Immunofluorescence of macrophages and YAP in the treatment and control groups. (c) and (d) Macrophage and YAP co-localization was analyzed in the treatment and control groups, with a closer fit indicating greater co-localization. (e) In the treatment groups, the co-localization of YAP and macrophages was more pronounced. The results are presented as means \pm SEM. * $p < 0.05$, ** $p < 0.01$, *** $p < 0.001$ vs. Control group ($n = 3$).

also be normalized after LIFU treatment (Fig. 4(e)). Follicle counting of the entire ovary by the hyalinization method similarly showed more antral follicles in the PCOS group and more primordial and mature follicles after LIFU treatment (Fig. 5(a)).

E. M1 AND M2 MACROPHAGES INTERACT WITH YAP IN GRANULOSA CELLS TO PROMOTE FOLLICULAR DEVELOPMENT IN RESPONSE TO LIFU TREATMENT

The iDISCO method was used to hyalinize the ovaries of the three groups of rats, and we counted the signal intensity

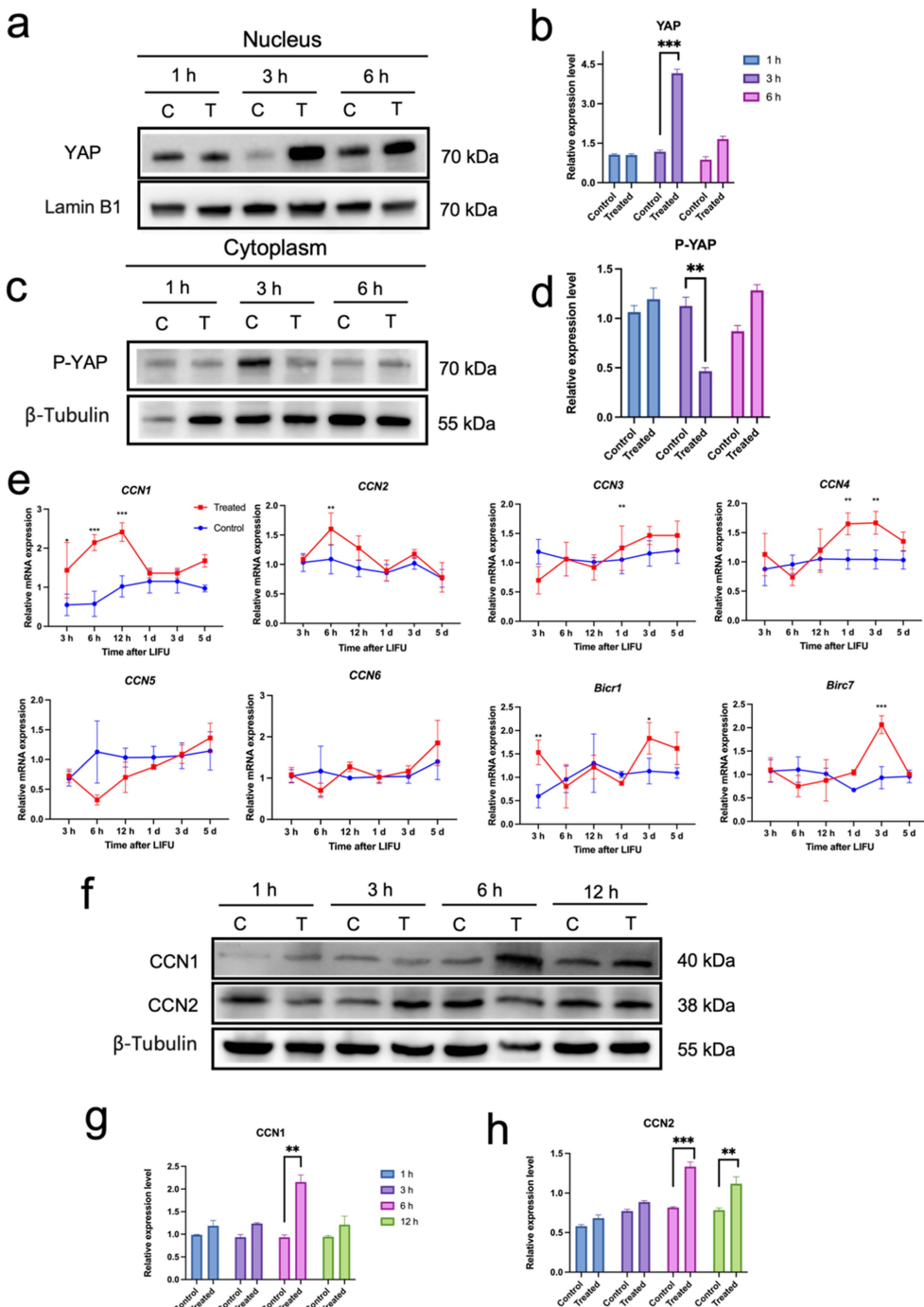


FIGURE 3. Mechanical effects of LIFU block the Hippo pathway and stimulate growth factor expression. (a) and (b) Nuclear YAP protein expression in granulocytes increased significantly at 3 h after LIFU stimulation. (c) and (d) Cytoplasmic P-YAP protein expression decreased at 3 h after LIFU stimulation. (e) CCN family mRNA expression changes. (f) CCN1 and CCN2 protein expression changes. (g) The expression of CCN1 protein was significantly up-regulated at 6 h after LIFU stimulation. (h) The expression of CCN2 protein was significantly up-regulated at 6 and 12 h after LIFU stimulation. Results are presented as means \pm SEM. * p < 0.05, ** p < 0.01, *** p < 0.001 vs. Control group ($n = 6$).

of macrophages in the rats' antral follicles. Our study found that macrophage signaling was less in the antral follicles of rats with PCOS-like compared to controls, and that LIFU treatment increased the number of macrophages in antral follicles (Fig. 5(b) and (c)). Furthermore, it was revealed that rats exhibiting PCOS characteristics and subjected to LIFU

treatment had greater numbers of mature follicles and corpora lutea (Fig. 5(a)). To further explore alterations in macrophage numbers and types, we further labeled M1 macrophages and M2 macrophages in the ovary. As shown in Fig. 6(a), our study found no noticeable difference in the numbers of M1 and M2 macrophages between the earlier and later stages of

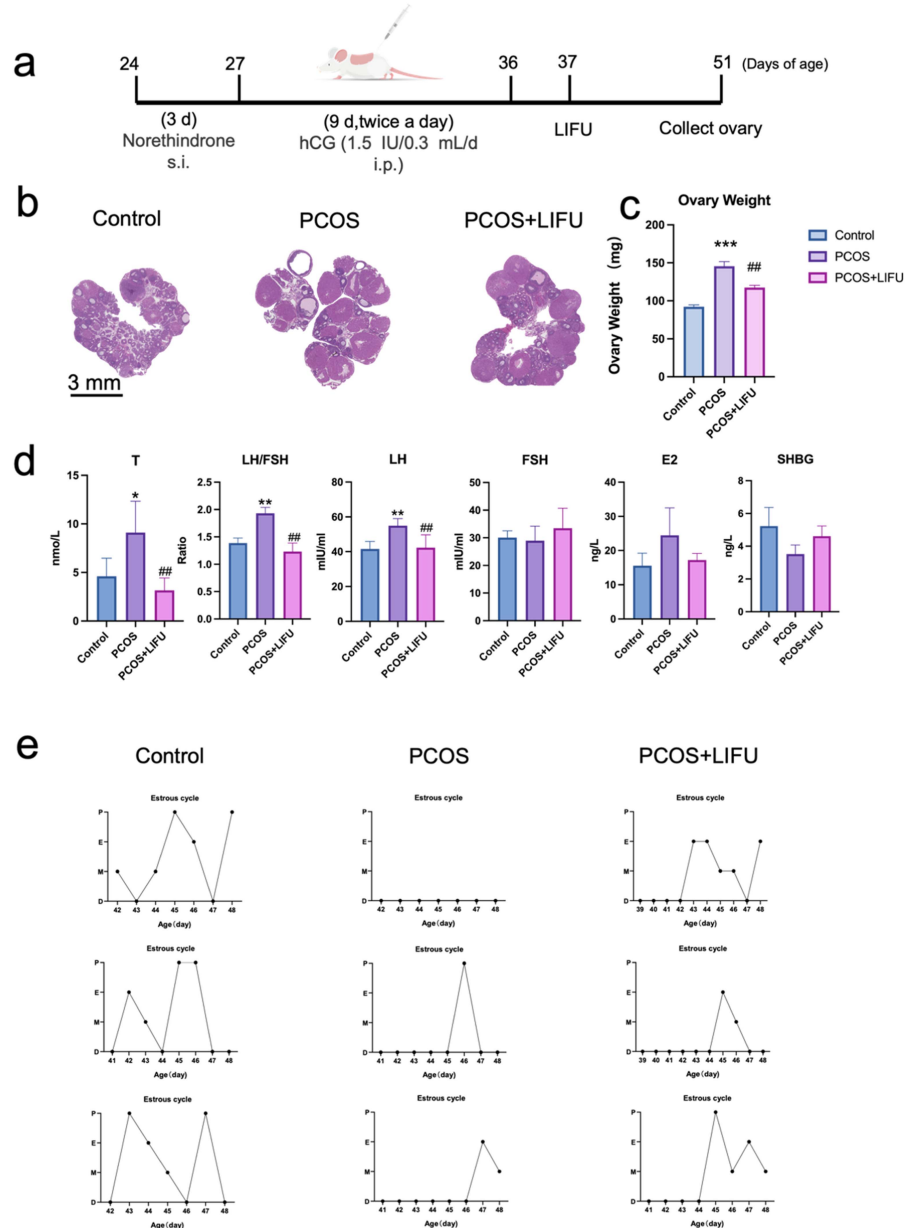


FIGURE 4. Increased antral follicles and disrupted hormone levels and motility cycles in PCOS-like rats can be reversed by LIFU. (a) Modeling of PCOS. (b) H&E staining of the control, PCOS, and PCOS+LIFU groups. (c) Weight of the control, PCOS, and LIFU groups. (d) Changes in the levels of testosterone (T), luteinizing hormone (LH), follicle stimulating hormone (FSH), estradiol (E2), and sex hormone binding globulin (SHBG) in the control, PCOS, and LIFU groups. (e) Motility cycle changes in the control, PCOS, and LIFU groups. Results are presented as means \pm SEM. *p < 0.05, **p < 0.01, ***p < 0.001 vs. Control group; #p < 0.05, ##p < 0.01 vs. PCOS group (n = 6).

follicle development in the ovaries of rats exhibiting symptoms similar to those of PCOS. Conversely, the antral follicles of the PCOS group demonstrated a substantial reduction in the quantity of M1 and M2 macrophages. Following LIFU treatment, the quantities of both macrophage types increased (Fig. 6(b)).

Consistent with the morphological changes, CCN1 and CCN2 protein levels were increased after LIFU treatment (Fig. 7(a) and (b)). We next looked at how the supernatant from macrophages that had been split into M1 and M2

phenotypes affected the amounts of YAP and CCN2 in granulosa cells. When compared to the direct stimulation of granulosa cells with LPS or IL-4, which showed no significant change (Fig. 7(e)–(f)), the expression of YAP and CCN2 was increased in ovarian granulosa cells by both M1 and M2 supernatants (Fig. 7(c) and (d)). TNF- α plays a role in facilitating the proliferation of mouse ovarian granulosa cells through the activation of the c-Jun signaling pathway [29], and this suggests that stimulation by LIFU induces a local immune response that can increase macrophage activation,

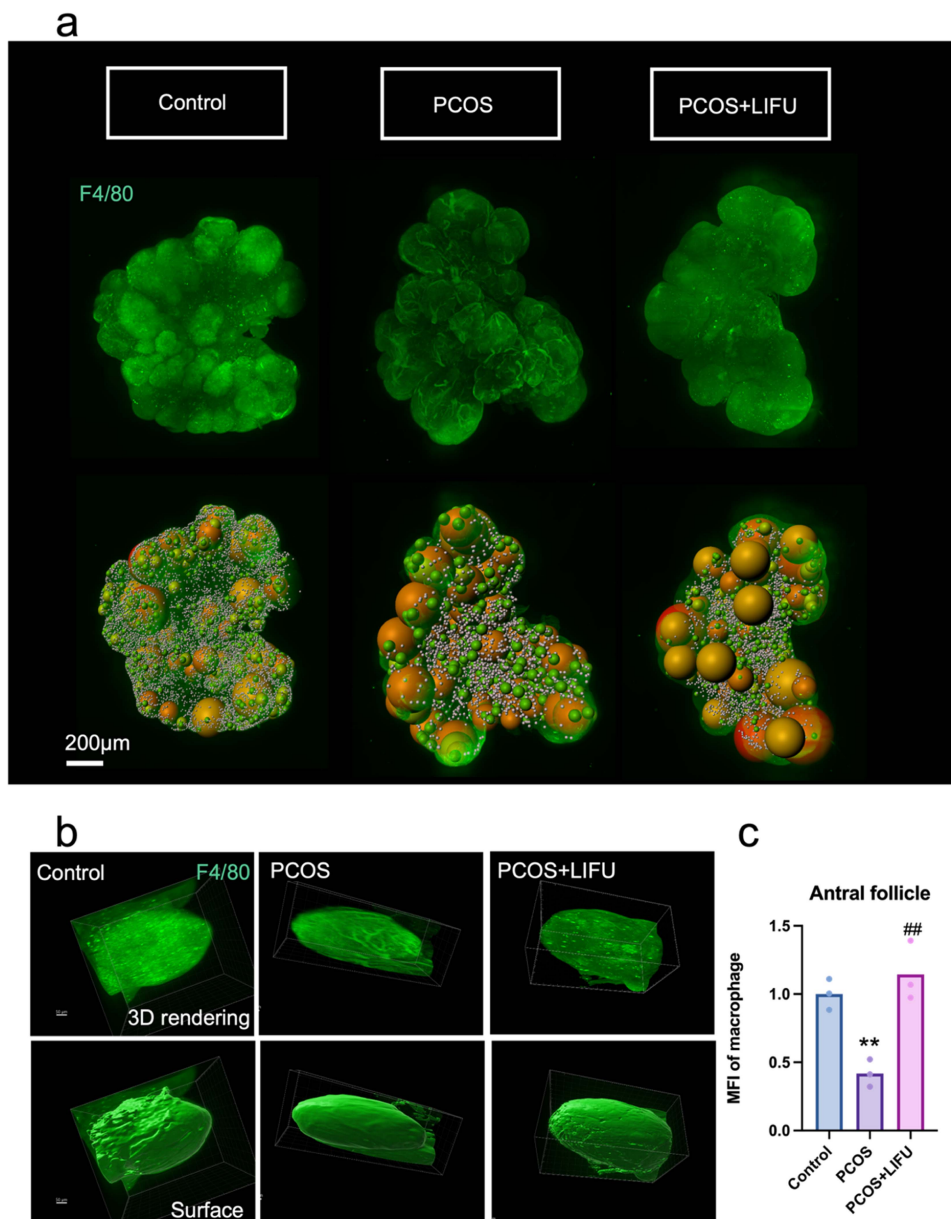


FIGURE 5. (a) Follicle counts at all stages in the Control, PCOS, and PCOS+LIFU groups (same method as before). (b) Expression of F4/80 (green) in the antral follicles of each group. (c) Mean fluorescence intensity (MFI) of F4/80 in the antral follicles. Results are presented as means \pm SEM. * p < 0.05vs. Control group; # p < 0.05, ## p < 0.01vs. PCOS group ($n = 3$).

and the secretion of a variety of inflammatory factors by macrophages can affect the expression of YAP and CCN2 in granulosa cells. In addition, LIFU inhibited the Hippo signaling pathway, resulting in enhanced translocation of YAP into the nucleus of granulosa cells. Consequently, this led to the activation of downstream alterations in CCN growth factors, thus facilitating the progression of follicular development. In PCOS, which is a model of chronic inflammation, various immune cells fail to play their proper roles, leading to stagnant development of antral follicles. LIFU can affect the local immune microenvironment, thus prompting the transformation

of macrophages into M1 or M2 classes in order to balance the anti-inflammatory and pro-inflammatory states.

III. DISCUSSION

For this work, we used a treatment parameter of 2 W LIFU due to its adequate mechanical impact in inducing structural modifications in the ovary while avoiding any harm caused by thermal effects. Our study found that LIFU can improve the growth of follicles by blocking the Hippo pathway and increasing the production of CCN family growth factors. In PCOS-like rats, LIFU could alter the population of M1 and

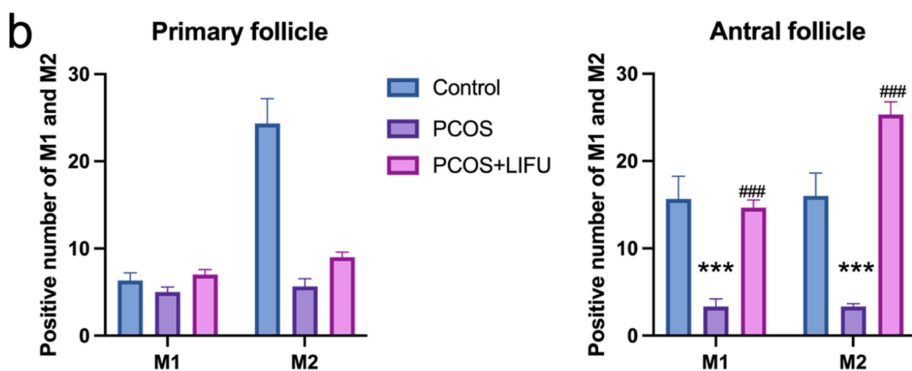
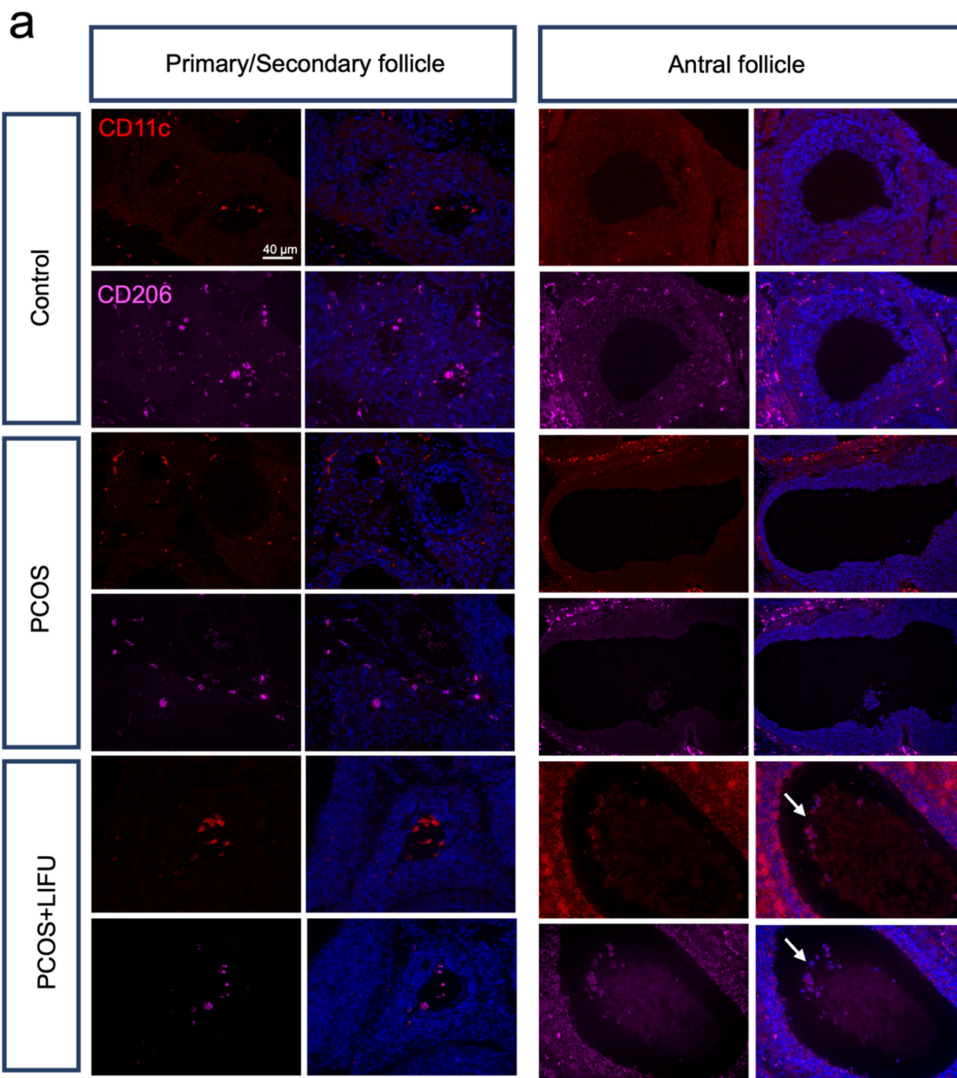


FIGURE 6. Changes in the numbers of M1 and M2 macrophages at different follicle stages. (a) Immunofluorescence staining of M1 (red) and M2 (magenta) macrophages in the three groups. (b) The numbers of M1 and M2 macrophages in the three groups. Results are presented as means \pm SEM. * p $<$ 0.05, ** p $<$ 0.01, *** p $<$ 0.001 vs. Control group; # p $<$ 0.05, ## p $<$ 0.01, ### p $<$ 0.001 vs. PCOS group (n = 3).

M2 macrophages in the ovary thus impacting the internal immunological environment and facilitating the progression of antral follicles towards maturation.

Focused ultrasound has great promise as an emerging non-invasive treatment. It is easy to use, practical, and has a bright

future in the medical industry. Furthermore, apart from its documented utilization in tumor therapy, this particular intervention also exhibits efficacy in the management of various other medical conditions by virtue of its impact on bone regeneration, neuromodulation, and the alleviation of chronic

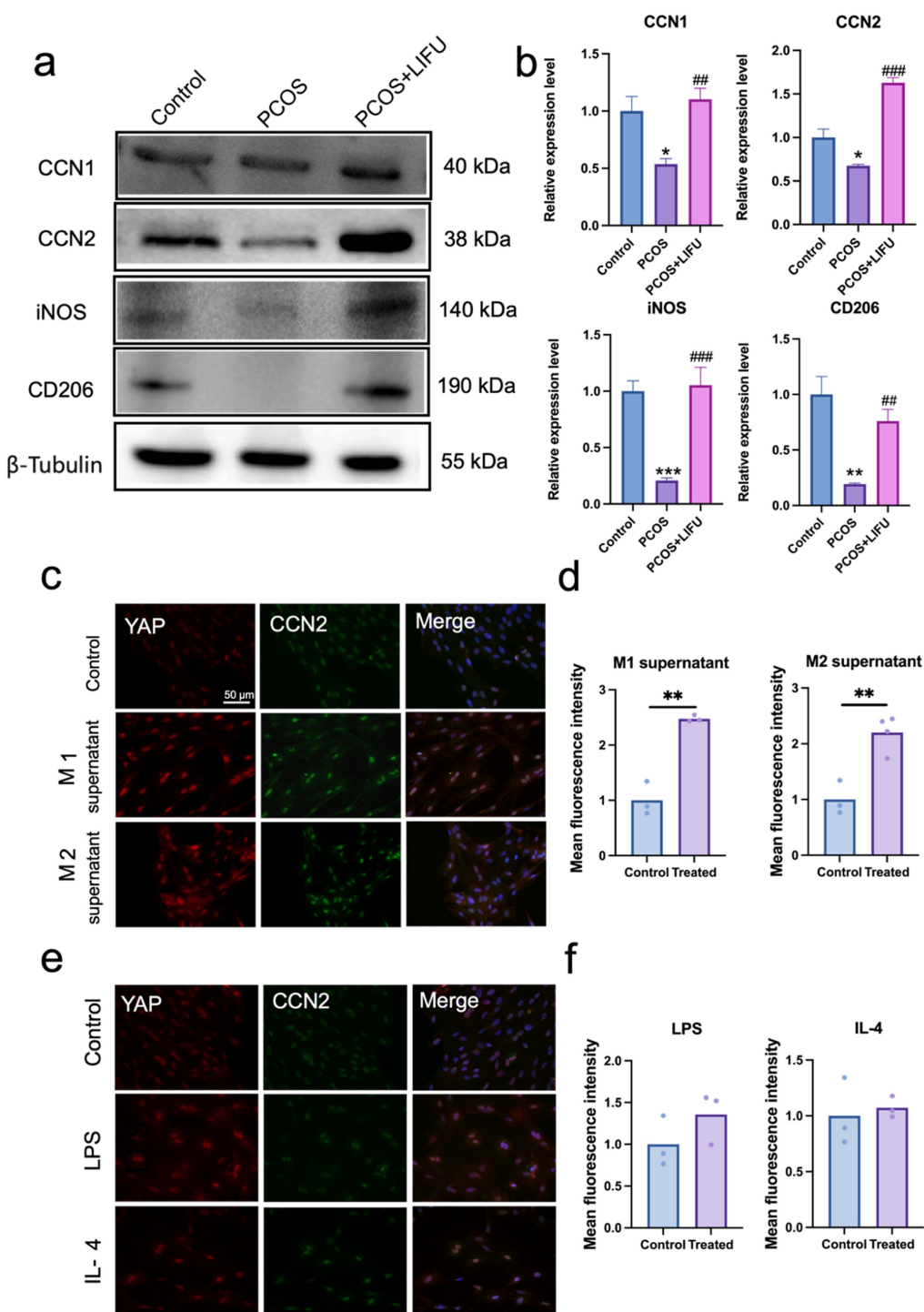


FIGURE 7. (a) and (b) CCN1, CCN2, iNOS, and CD206 protein expression in the control, PCOS, and PCOS+LIFU groups. (c) and (d) Immunofluorescence staining of YAP and CCN2 after stimulation of granulocytes with supernatants from M1 and M2 macrophages. (e) and (f) Negative control showing that the M1 and M2 macrophage-inducing drugs LPS and IL-4 acted directly on granulocytes. Results are presented as means \pm SEM. * $p < 0.05$, ** $p < 0.01$, *** $p < 0.001$ vs. Control group; # $p < 0.05$, ## $p < 0.01$, ### $p < 0.001$ vs. PCOS group ($n = 3$).

pain [30]. LIFU is much safer than HIFU, and studies have shown that LIFU has minimal thermal effects when applied to tissues and thus does not cause tissue damage [31].

PCOS is a significant etiological factor contributing to female infertility; however, despite many breakthroughs

in treatments, including drugs and surgeries, reproductive medicine practitioners are still focused on developing non-invasive and cost-effective treatments. Thus there is an emerging use of LIFU therapy in obstetrics and gynecology in addition to the widely used clinical application of HIFU.

The Hippo pathway is blocked by mechanical disruption of cellular structures, and the mechanical stimulation from ultrasound has strong effects on the local immune response. Consequently, the present work was focused on investigating the Hippo pathway and its impact on alterations in macrophages. Under physiologic conditions, we found that the application of LIFU could induce mature follicles in the ovaries of immature rats, and the possible mechanism was that YAP entry into the nucleus after 3 h of LIFU caused an increase in the expression of downstream CCN family proteins. In contrast, under pathological conditions in the PCOS model an atypical augmentation in macrophage populations was noted as a consequence of the persistent inflammatory condition associated with the disease. Macrophages exhibit a remarkable degree of plasticity, and they possess the ability to develop into several subtypes and subsequently perform diverse biological roles upon exposure to varied environmental stimuli [32], [33]. Many studies have shown that macrophages function by releasing signaling molecules in ovarian tissue and that they are important helper cells in achieving fertility [34], [35], and during both the pre-ovulatory and the inter-ovulatory phase there is a discernible increase in the number of ovarian macrophages in mice [36], [37]. In murine models, the population of M1 macrophages increases to a maximum level during ovulation. Specifically, M1 macrophages are observed in the vicinity of ovulating follicles, while M2 macrophages are predominantly present in the vicinity of developing follicles [38]. The work of Fukumatsu suggests that co-culture of mouse granulocytes with peritoneal macrophages leads to the proliferation of granulocytes [39], and studies have shown that macrophages are capable of releasing a substantial amount of cytokines that have a pivotal effect in the ovulation process, with specific emphasis on IL-1 β and TNF- α [40], [41]. A further investigation demonstrated that the introduction of intracapsular clodronate liposomes in mice led to a reduction in the frequency of ovulation and a postponement of the estrus cycle by removing ovarian macrophages [42].

Increasing evidence indicates that macrophages and the products that are released from macrophages are involved in a variety of ovarian dysfunctions, particularly in PCOS [43], and disproportionate ratios of M1 and M2 macrophages are often observed in models of PCOS [44], [45]. During the course of the current experiment, it was discovered that the PCOS model exhibited a decrease in the quantity of macrophages of both the M1 and M2 types, and LIFU stimulation could reverse this situation. However, it has been reported in the literature that M2 macrophages are decreased in the PCOS model, while M1 macrophages are increased [46], [47]. We speculate that this discrepancy may be due to different modeling methods. This phenomenon occurs due to the presence of hyperandrogenemia, which serves to maintain a delicate equilibrium between pro-inflammatory and anti-inflammatory signals. In addition, hyperandrogenemia promotes the polarization of macrophages in the peripheral and ovarian regions towards the M1 phenotype. It

also triggers the release of pro-inflammatory substances and impacts the ovaries by increasing the presence of CMKLR1-positive M1 macrophages [48]. Macrophage-secreted TNF- α promotes mouse ovarian granulosa cell proliferation via the c-Jun signaling pathway [29], and animals with a deletion of the TNF- α gene show increased proliferation of granulosa cells and reduced death of oocytes [49]. In the present work we studied granulosa cells and showed that the key inflammatory components that were produced by M1 and M2 macrophages were also capable of up-regulating the expression of YAP and CCN2, thus further promoting follicular development. The physiological environment within living organisms is characterized by a delicate equilibrium between pro- and anti-inflammatory signals. The reciprocal regulation between local macrophages and environmental signals plays a significant role in orchestrating the allocation of M1 and M2 macrophages, ultimately leading to the establishment of homeostasis [50], [51], and pathological circumstances are the result of a disruption in this equilibrium.

LIFU is a treatment technique that has shown efficacy in facilitating the healing process of several medical conditions, including surgical incisions, fractures, tendon injuries, and nerve injuries. This therapeutic approach is characterized by its safety, cost-effectiveness, and convenience [52]. Numerous studies have shown the neuroprotective and reversible neuro-modulatory effects of LIFU both *in vitro* and *in vivo* [53], [54]. Eguchi et al. found that the use of whole-brain LIPUS therapy yielded positive outcomes in ameliorating cognitive impairments in mouse models of dementia, and they found a significant increase in CD31-positive endothelial cells along with Olig2-positive oligodendrocyte precursor cells in a model of vascular dementia following LIPUS therapy. Additionally, LIPUS treatment led to a reduction in Iba-1-positive microglial cells and amyloid- β plaques in a model of Alzheimer's disease [55]. An additional domain of interest is the management of periodontal disease, wherein LIPUS has demonstrated efficacy in facilitating the regeneration of both root and periodontal tissues [56].

The shortcomings of this study are mainly due to the fact that YAP, a key transcription factor, was not knocked down in order to determine whether the effect of LIFU was lost. Secondly, PCOS-like rats were not mated to see if the number of offspring could be increased after LIFU treatment. Additional comprehensive investigations are thus required to confirm the impacts of LIFU on the female reproductive system.

IV. CONCLUSION

The mechanical impact of LIFU has the potential to induce alterations in the internal architecture and arrangement of the ovary, thus influencing the Hippo pathway and facilitating the progression of follicular growth and development. Additionally, LIFU has the capacity to modify the proportion of M1 macrophages to M2 macrophages, thus facilitating the progression of antral follicles towards mature follicles in the

context of the chronic inflammation observed in PCOS-like rats.

V. MATERIALS AND METHODS

A. ANIMALS

The rats were maintained in a controlled environment, which included a 12 h light/dark cycle, a constant temperature of 22 ± 2 °C, and a humidity range of 45–55 %. They were provided with unrestricted access to food and water. Ten-day-old female Wistar rats with a breastfeeding mother (Shanghai SLAC Laboratory Animal Co., Ltd., Shanghai, China) were subjected to LIFU stimulation under anesthesia. The ovary on one side of the animal was treated, and at the end of the procedure the ovary on the other side of the animal was injected with 10 IU of PMSG as a control. The ovaries were collected and weighed after 5 days. For the model of PCOS, 24 immature female Wistar rats, which were 24 days old and had an average body weight of 60 ± 5 g, were chosen for the study. The rats were chosen at random and placed into one of three groups: Control, PCOS, and PCOS+LIFU ($n = 8$ per group). The PCOS model was established with reference to the literature [57], [58]. The experimental groups were implanted with 18-methylkynurenine silica gel rods 3 mm subcutaneously at the age of 24 days, containing approximately 5 mg of 18-methylkynurenine (each rod was 4.4 cm long and 2.4 mm in diameter, containing 75 mg of levulinic 18-methylkynurenine, Shanghai Dahua Pharmaceutical Plant). At 27 days of age, 1.5 IU hCG (30 µl) was injected subcutaneously, bid $\times 9$ d. The normal control group received a subcutaneous injection of the same volume of saline as the other groups. The LIFU group was treated with ultrasound at the end of the modeling, and the location of the treatment was bilateral ovaries. Rats were sacrificed after two weeks of observation.

B. LIFU TREATMENT

Rats were shaved in the dorsal ovary region under gas anesthesia (RMAS-100921001, Raymai, China), and the dorsal skin was incised after sterilization. Before the ultrasound treatment, the rat was put into the induction box that was filled with isoflurane (4 cc/min with an airflow rate of 6 cc/min). An anesthesia mask was used to cover the mouth and nose of the rat, and the anesthesia was adjusted to a dosage of 2–3 cc/min. The rat ovary was gently pulled out and placed under the center of the ultrasound instrument probe (USR-2; Chongqing Haifu Medical Technology Co Ltd., Chongqing, China), and the treatment parameters were 200 J for 100 s (each pulse had a sonication time of 1 s and a cooling time of 2 s). At the end of the treatment, the ovary was returned to its original position and the skin was sutured with sterile sutures. The parameters of the LIFU device were set as follows: spatial peak-temporal average intensity = 42.32 W/cm²; exposure time = 100 s (in pulses of sonication time 1 s and cooling time 2 s); frequency = 650 kHz; duty cycle = 13 %; acoustic power = 2 W, 4 W, or 8 W.

C. ESTROUS CYCLE

Regular vaginal smears were taken every day between 4 p.m. and 5 p.m. for microscopic examination to identify the predominant cell type and thus ascertain the stage of the estrous cycle. Round nucleated epithelial cells were seen during the proestrus phase, cornified squamous epithelial cells indicated the estrus phase, the simultaneous presence of leukocytes and nucleated epithelial cells indicated the diestrus phase, and the coexistence of leukocytes and nucleated epithelial cells indicated the metestrus phase.

D. HORMONE PROFILE

Before the rats were sacrificed, serum samples were collected from the abdominal aorta. These samples were stored at -80 °C until they were analyzed using an ELISA to determine the levels of 17β -estradiol, follicle-stimulating hormone, luteinizing hormone, progesterone, testosterone, and sex hormone binding globulin (Supplementary material: Table S1). The levels of endogenous hormones and cholesterol were measured using radioimmunoassay and colorimetric kits on a microplate reader (SpectraMax Paradigm, Molecular Devices) in accordance with the instructions provided by the manufacturers. Each sample was analyzed in duplicate.

E. QUANTITATIVE REAL-TIME PCR ANALYSIS

Following the manufacturer's instructions, the extraction of total RNA from ovarian tissue was carried out using Trizol reagent. Prime Script RT Master Mix was then used to generate single-stranded cDNA from every sample with an average yield of 2 µg. The qRT-PCR was performed using an ABI PRISM 7300 sequence detection system. Following the manufacturer's recommendations for PCR settings, amplifications were conducted using a SYBR Premix Ex Taq kit. All reactions were carried out in triplicate on 96-well plates, and all primers were analyzed to ensure that the target gene was homogeneous. The dissociation curve of the qRT-PCR test provided additional evidence of the primer's quality before use. The primer sequences for *CCN1*, *CCN2*, *CCN3*, *CCN4*, *CCN5*, *CCN6*, *BIRC1*, and *BIRC7* are listed in Supplementary material: Table S2. The $2^{-\Delta\Delta Ct}$ method was used to assess the relative expression levels of the target genes with *GAPDH* acting as the internal reference.

F. IMMUNOFLOURESCENCE STAINING

Ovarian granulosa cells were immersed in a 4% paraformaldehyde solution for 15 minutes along with 0.1% Triton X-100 to disrupt the cell membranes, and this was followed by blocking with 5% BSA. The samples were incubated with primary antibodies against YAP and CTGF overnight at 4 °C, and the nuclei were labeled with DAPI. Immunofluorescence staining of ovarian tissues was performed to analyze macrophage polarization. Briefly, 4 µm paraffin sections were sequentially deparaffinized, antigenically repaired by a citrate-based antigen retrieval solution, washed with PBS, permeabilized with 0.1% Triton X-100, blocked in 5% BSA,

and incubated with primary and secondary antibodies. The rabbit polyclonal anti-CD206 primary antibody was used to identify M2 macrophages, and rabbit monoclonal anti-CD11c primary antibody was used to identify M1 macrophages. The samples were then incubated with Alexa Fluor 561 anti-rabbit IgG and Alexa Fluor 647 anti-rabbit IgG secondary antibodies. Hematoxylin and eosin (H&E) staining was performed in accordance with the documented protocol on 4 µm slices derived from ovarian tissue that had undergone fixation in 4% paraformaldehyde for a duration of 24 hours followed by embedding in paraffin. The specimens were examined using a fluorescence microscope (BZ-X810 All-in-one Fluorescence Microscope, Olympus Corporation, Tokyo, Japan) outfitted with four lasers emitting at wavelengths of 405 nm, 488 nm, 561 nm, and 647 nm. All antibody information in Supplementary material: Table S3.

G. WESTERN BLOTTING

RIPA lysis buffer was used to extract protein from the cells and tissue, and a BCA kit was used to determine the amount of protein that was extracted. The protein samples were diluted to a uniform concentration using loading buffer, and they were stored at -80 °C until being examined. The proteins were separated by SDS-PAGE and then transferred to polyvinylidene fluoride membranes and treated with primary and secondary antibodies. When required, a Western blot stripping buffer was added for 30 minutes at room temperature to obtain the membranes. The samples were washed three times in TBST and then refracted again. The protein bands were identified using ImageQuant LAS4000 mini-gel imaging technology. Image-Pro Plus 6.0 was used for standardizing and assessing the protein band densities with β-tubulin acting as the loading control.

H. iDISCO AND 3D IMAGING ANALYSIS

We used the revised iDISCO technique in our investigation [59]. The rats were fully sedated using 20% urethane and then subjected to cardiopulmonary perfusion with ice-cold 0.9% saline and 4% paraformaldehyde. After being postfixed overnight at 4 °C, each sample was rinsed three times for one hour at room temperature with 1× PBS. Following a 1-hour dehydration at room temperature in gradient methanol, the samples were incubated in 100% methanol for three hours. After that, the samples were bleached overnight at 4 °C using 5% H₂O₂ in 20% DMSO/methanol and then rehydrated in 100%, 80%, 60%, 40%, and 20% methanol. The samples were subsequently immersed in PBS for one hour followed by two further washes using a solution consisting of 0.2% Triton X-100 in PBS. The samples were then incubated at 37 °C for a maximum of two days in permeabilization and blocking solutions followed by immunolabeling with primary antibodies. Following this, the samples underwent a one-day washing step in a solution containing PBS, 0.2% Tween-20, and 10 mg/ml heparin. The samples underwent dehydration using methanol solutions with concentrations of 20%, 40%, 60%, 80%, and 100% for a duration of one hour each. A

secondary antibody diluent was used to incubate the samples for the specified amount of time before this step was taken. The samples were subsequently immersed in a solution of PBS, 0.2% Tween-20, and 10 mg/ml of heparin for one day. The samples were then incubated for three hours in a solution consisting of 66% dichloromethane and then washed twice for 15 min each in 100% dichloromethane to eliminate any residual methanol. Finally, the samples were immersed in dibenzyl ether and stored in the solvent at room temperature.

The cleaned ovarian tissues were photographed using a light-sheet microscope with 6.3× magnification and 1 × objective. The 3D images were examined and rebuilt using Imaris software, and the follicles were semi-manually identified using the Imaris Spot method.

I. STATISTICAL ANALYSIS

The data are shown as the mean and the standard error of the mean. We used either a one-way analysis of variance (ANOVA) or a two-way ANOVA combined with Tukey's test to conduct statistical analysis on data that was collected from three separate groups. Prism 9.5.0 (GraphPad Software) was used for all analyses, and p-values <0.05 were considered significant.

I. SUPPLEMENTARY MATERIALS

Supplementary material includes reagents and primers used in the text.

ACKNOWLEDGMENT

The contributions of professors Aaron J.W. Hsueh to this research are much appreciated. The authors acknowledge the support of Neurobiology's Core Facility for Large-Scale Tissue Clearing and Data Analysis for their 3D image analysis and Basic Medical Sciences' Department of Integrative Medicine of Fudan University School. The authors express their gratitude to Man Luo from Chongqing Haifu Medical Technology Co., Ltd. for providing technical support in the use of the LIFU exposure equipment.

Author Contributions: The experiments were conceptualized and designed by Y.F., A.H., Y.X., L.Y., and Y.X. Additionally, they were responsible for developing the project procedures and establishing collaborations. The experiments were conducted by Y.X., Y.W., Y.W., Y.C., W.L., Z.P., and R.Z. The data were analyzed by Y.X. The manuscript was authored by Y.X. and Y.F.. A.H. and Y.X. contributed to the scientific supervision, offered assistance, and made editorial revisions to the paper. Y.X., and Y.F. are acknowledged as the guarantors of this study, indicating that they were granted complete access to all the data and are accountable for maintaining the data's integrity and verifying the precision of the data analysis. All of the writers have read and approved the final article.

Ethics Approval: The Chinese National Institutes of Health's Guide for the Care and Use of Laboratory Animals was followed for all animal experiments. The local ethics committee of Shanghai Medical College, Fudan University, gave its approval to the study.

Competing Interests: The authors assert that they have no conflicts of interest.

REFERENCES

- [1] S. Golezar, F. Ramezani Tehrani, S. Khazaei, A. Ebadi, and Z. Keshavarz, "The global prevalence of primary ovarian insufficiency and early menopause: A meta-analysis," *Climacteric*, vol. 22, no. 4, pp. 403–411, 2019.
- [2] A. L. G. Notaro and F. T. L. Neto, "The use of metformin in women with polycystic ovary syndrome: An updated review," *J. Assist. Reproduction Genet.*, vol. 39, no. 3, pp. 573–579, 2022.
- [3] K. Lejman-Larysz et al., "Influence of vitamin D on the incidence of metabolic syndrome and hormonal balance in patients with polycystic ovary syndrome," *Nutrients*, vol. 15, no. 13, 2023, Art. no. 2952.
- [4] K. Kawamura et al., "Hippo signaling disruption and Akt stimulation of ovarian follicles for infertility treatment," *Proc. Nat. Acad. Sci.*, vol. 110, no. 43, pp. 17474–17479, 2013.
- [5] C. L. Chang, "Facilitation of ovarian response by mechanical force—Latest insight on fertility improvement in women with poor ovarian response or primary ovarian insufficiency," *Int. J. Mol. Sci.*, vol. 24, no. 19, 2023, Art. no. 14751.
- [6] X. Zhang, T. Han, L. Yan, X. Jiao, Y. Qin, and Z.-J. Chen, "Resumption of ovarian function after ovarian biopsy/scratch in patients with premature ovarian insufficiency," *Reprod. Sci.*, vol. 26, no. 2, pp. 207–213, 2019.
- [7] D. L. Miller et al., "Overview of therapeutic ultrasound applications and safety considerations," *J. Ultrasound Med.*, vol. 31, no. 4, pp. 623–634, 2012.
- [8] J. E. Kennedy, "High-intensity focused ultrasound in the treatment of solid tumours," *Nature Rev. Cancer*, vol. 5, no. 4, pp. 321–327, 2005.
- [9] C. M. Tempany, N. J. McDannold, K. Hyynnen, and F. A. Jolesz, "Focused ultrasound surgery in oncology: Overview and principles," *Radiology*, vol. 259, no. 1, pp. 39–56, 2011.
- [10] G. R. Ter Haar, "High intensity focused ultrasound for the treatment of tumors," *Echocardiography*, vol. 18, no. 4, pp. 317–322, 2001.
- [11] O. Al-Bataineh, J. Jenne, and P. Huber, "Clinical and future applications of high intensity focused ultrasound in cancer," *Cancer Treat. Rev.*, vol. 38, no. 5, pp. 346–353, 2012.
- [12] L. Yan, H. Huang, J. Lin, and R. Yu, "High-intensity focused ultrasound treatment for symptomatic uterine fibroids: A systematic review and meta-analysis," *Int. J. Hyperthermia*, vol. 39, no. 1, pp. 230–238, 2022.
- [13] J. Rabinovici et al., "Pregnancy outcome after magnetic resonance-guided focused ultrasound surgery for conservative treatment of uterine fibroids," *Obstet. Gynecol. Surv.*, vol. 65, no. 5, pp. 316–318, 2010.
- [14] M. Zou, L. Chen, C. Wu, C. Hu, and Y. Xiong, "Pregnancy outcomes in patients with uterine fibroids treated with ultrasound-guided high-intensity focused ultrasound," *BJOG Int. J. Obstet. Gynaecol.*, vol. 124, pp. 30–35, 2017.
- [15] N. S. Abtahi et al., "Effect of therapeutic ultrasound on folliculogenesis, angiogenesis and apoptosis after heterotopic mouse ovarian transplantation," *Ultrasound Med. Biol.*, vol. 40, no. 7, pp. 1535–1544, 2014.
- [16] X.-M. Xu et al., "Low-intensity pulsed ultrasound treatment accelerates angiogenesis by activating YAP/TAZ in human umbilical vein endothelial cells," *Ultrasound Med. Biol.*, vol. 44, no. 12, pp. 2655–2661, 2018.
- [17] H. Tang, Y. Liu, Y. Fan, and C. Li, "Therapeutic effects of low-intensity pulsed ultrasound on premature ovarian insufficiency," *Ultrasound Med. Biol.*, vol. 47, no. 8, pp. 2377–2387, 2021.
- [18] A. G. Moussatov, A. C. Baker, and F. A. Duck, "A possible approach to the treatment of polycystic ovarian syndrome using focused ultrasound," *Ultrasonics*, vol. 36, no. 8, pp. 893–900, 1998.
- [19] I. A. Shehata, J. R. Ballard, A. J. Casper, L. J. Hennings, E. Cressman, and E. S. Ebbini, "High-intensity focused ultrasound for potential treatment of polycystic ovary syndrome: Toward a noninvasive surgery," *Fertility. Sterility*, vol. 101, no. 2, pp. 545–551, 2014.
- [20] J. Qin et al., "Low-intensity pulsed ultrasound promotes repair of 4-vinylcyclohexene diepoxide-induced premature ovarian insufficiency in SD rats," *J. Gerontol. Ser. A*, vol. 77, no. 2, pp. 221–227, 2022.
- [21] U. Daood and A. S. Fawzy, "Macrophage response and surface analysis of dental cementum after treatment with high intensity focused ultrasound," *Arch. Oral Biol.*, vol. 98, pp. 195–203, 2019.
- [22] K. Schregel et al., "Targeted blood brain barrier opening with focused ultrasound induces focal macrophage/microglial activation in experimental autoimmune encephalomyelitis," *Front. Neurosci.*, vol. 15, 2021, Art. no. 665722.
- [23] Y. Zhang et al., "Molecular identity changes of tumor-associated macrophages and microglia after magnetic resonance imaging-guided focused ultrasound-induced blood-brain barrier opening in a mouse glioblastoma model," *Ultrasound Med. Biol.*, vol. 49, no. 5, pp. 1082–1090, 2023.
- [24] F.-X. Yu, B. Zhao, and K.-L. Guan, "Hippo pathway in organ size control, tissue homeostasis, and cancer," *Cell*, vol. 163, no. 4, pp. 811–828, 2015.
- [25] F.-X. Yu and K.-L. Guan, "The Hippo pathway: Regulators and regulations," *Genes Develop.*, vol. 27, no. 4, pp. 355–371, 2013.
- [26] S. Ma, Z. Meng, R. Chen, and K.-L. Guan, "The Hippo pathway: Biology and pathophysiology," *Annu. Rev. Biochem.*, vol. 88, pp. 577–604, 2019.
- [27] Z. Meng, T. Moroishi, and K.-L. Guan, "Mechanisms of Hippo pathway regulation," *Genes Dev.*, vol. 30, no. 1, pp. 1–17, 2016.
- [28] K. F. Harvey, X. Zhang, and D. M. Thomas, "The Hippo pathway and human cancer," *Nature Rev. Cancer*, vol. 13, no. 4, pp. 246–257, 2013.
- [29] D.-S. Son, K. Y. Arai, K. F. Roby, and P. F. Terranova, "Tumor necrosis factor α (TNF) increases granulosa cell proliferation: Dependence on c-Jun and TNF receptor type 1," *Endocrinology*, vol. 145, no. 3, pp. 1218–1226, 2004.
- [30] A. Bystritsky et al., "A review of low-intensity focused ultrasound pulsation," *Brain Stimulation*, vol. 4, no. 3, pp. 125–136, 2011.
- [31] S. B. Tajali, P. Houghton, J. C. MacDermid, and R. Grewal, "Effects of low-intensity pulsed ultrasound therapy on fracture healing: A systematic review and meta-analysis," *Amer. J. Phys. Med. Rehabil.*, vol. 91, no. 4, pp. 349–367, 2012.
- [32] A. Shapouri-Moghadam et al., "Macrophage plasticity, polarization, and function in health and disease," *J. Cell. Physiol.*, vol. 233, no. 9, pp. 6425–6440, 2018.
- [33] A. Sica and A. Mantovani, "Macrophage plasticity and polarization: In vivo veritas," *J. Clin. Invest.*, vol. 122, no. 3, pp. 787–795, 2012.
- [34] P. E. Cohen, K. Nishimura, L. Zhu, and J. W. Pollard, "Macrophages: Important accessory cells for reproductive function," *J. leukocyte Biol.*, vol. 66, no. 5, pp. 765–772, Nov. 1999, doi: [10.1002/jlb.66.5.765](https://doi.org/10.1002/jlb.66.5.765).
- [35] R. J. Norman and M. Brännstrom, "White cells and the ovary—incidental invaders or essential effectors?" *J. Endocrinol.*, vol. 140, no. 3, pp. 333–336, 1994.
- [36] M. Brännström, G. Mayrhofer, and S. A. Robertson, "Localization of leukocyte subsets in the rat ovary during the periovulatory Period," *Biol. Reproduction*, vol. 48, no. 2, pp. 277–286, Feb. 1993, doi: [10.1093/biolreprod48.2.277](https://doi.org/10.1093/biolreprod48.2.277).
- [37] M. Petrovská, D. G. Dimitrov, and S. D. Michael, "Quantitative changes in macrophage distribution in normal mouse ovary over the course of the estrous cycle examined with an image analysis system," *Amer. J. Reprod. Immunol.*, vol. 36, no. 3, pp. 175–183, Sep. 1996, doi: [10.1111/j.1600-0897.1996.tb00159.x](https://doi.org/10.1111/j.1600-0897.1996.tb00159.x).
- [38] Y. Xiao et al., "Macrophage-derived extracellular vesicles regulate follicular activation and improve ovarian function in old mice by modulating local environment," *Clin. Transl. Med.*, vol. 12, no. 10, Oct. 2022, Art. no. e1071, doi: [10.1002/ctm2.1071](https://doi.org/10.1002/ctm2.1071).
- [39] Y. Fukumatsu, H. Katabuchi, M. Naito, M. Takeya, K. Takahashi, and H. Okamura, "Effect of macrophages on proliferation of granulosa cells in the ovary in rats," *Reproduction*, vol. 96, no. 1, pp. 241–249, 1992.
- [40] E. Y. Adashi, "The potential role of interleukin-1 in the ovulatory process: An evolving hypothesis," *Mol. Cell. Endocrinol.*, vol. 140, no. 1/2, pp. 77–81, 1998.
- [41] M. Brännstrom, N. Bonello, L. J. Wang, and R. J. Norman, "Effects of tumour necrosis factor alpha (TNF alpha) on ovulation in the rat ovary," *Reproduction Fertility Develop.*, vol. 7, no. 1, pp. 67–73, 1995.
- [42] K. H. Van der Hoek, S. Maddocks, C. M. Woodhouse, N. van Rooijen, S. A. Robertson, and R. J. Norman, "Intrabursal injection of clodronate liposomes causes macrophage depletion and inhibits ovulation in the mouse Ovary1," *Biol. Reproduction*, vol. 62, no. 4, pp. 1059–1066, Apr. 2000, doi: [10.1093/biolreprod62.4.1059](https://doi.org/10.1093/biolreprod62.4.1059).
- [43] Y. Feng, Z. Tang, and W. Zhang, "The role of macrophages in polycystic ovarian syndrome and its typical pathological features: A narrative review," *Biomed. Pharmacother.*, vol. 167, 2023, Art. no. 115470.

- [44] F. Figueroa, R. Davicino, B. Micalizzi, L. Oliveros, and M. Forneris, “Macrophage secretions modulate the steroidogenesis of polycystic ovary in rats: Effect of testosterone on macrophage pro-inflammatory cytokines,” *Life Sci.*, vol. 90, no. 19–20, pp. 733–739, 2012.
- [45] X. Li, L. Li, D. Ouyang, Y. Zhu, and T. Yuan, “The abnormal expression of kisspeptin regulates pro-inflammatory cytokines, cell viability and apoptosis of macrophages in hyperandrogenism induced by testosterone,” *Gynecol. Endocrinol.*, vol. 37, no. 1, pp. 72–77, Jan. 2021, doi: [10.1080/09513590.2020.1811964](https://doi.org/10.1080/09513590.2020.1811964).
- [46] Y. Luan, L. Zhang, Y. Peng, Y. Li, R. Liu, and C. Yin, “Immune regulation in polycystic ovary syndrome,” *Clin. Chimica Acta*, vol. 531, pp. 265–272, 2022.
- [47] S. Tedesco et al., “Activation profiles of monocyte-macrophages and HDL function in healthy women in relation to menstrual cycle and in polycystic ovary syndrome patients,” *Endocrine*, vol. 66, no. 2, pp. 360–369, Nov. 2019, doi: [10.1007/s12020-019-01911-2](https://doi.org/10.1007/s12020-019-01911-2).
- [48] C. Su, M. Chen, H. Huang, and J. Lin, “Testosterone enhances lipopolysaccharide-induced interleukin-6 and macrophage chemotactic protein-1 expression by activating the extracellular signal-regulated kinase 1/2/nuclear factor- κ b signalling pathways in 3T3-L1 adipocytes,” *Mol. Med. Rep.*, vol. 12, no. 1, pp. 696–704, 2015.
- [49] L. Cui, G. Yang, J. Pan, and C. Zhang, “Tumor necrosis factor α knockout increases fertility of mice,” *Theriogenology*, vol. 75, no. 5, pp. 867–876, 2011.
- [50] Y. Lavin et al., “Tissue-resident macrophage enhancer landscapes are shaped by the local microenvironment,” *Cell*, vol. 159, no. 6, pp. 1312–1326, 2014.
- [51] D. Gosselin et al., “Environment drives selection and function of enhancers controlling tissue-specific macrophage identities,” *Cell*, vol. 159, no. 6, pp. 1327–1340, 2014.
- [52] X. Jiang et al., “A review of low-intensity pulsed ultrasound for therapeutic applications,” *IEEE Trans. Biomed. Eng.*, vol. 66, no. 10, pp. 2704–2718, Oct. 2019.
- [53] Y. Tufail et al., “Transcranial pulsed ultrasound stimulates intact brain circuits,” *Neuron*, vol. 66, no. 5, pp. 681–694, 2010.
- [54] F. J. Fry, H. W. Ades, and W. J. Fry, “Production of reversible changes in the central nervous system by ultrasound,” *Science*, vol. 127, no. 3289, pp. 83–84, 1958.
- [55] K. Eguchi et al., “Whole-brain low-intensity pulsed ultrasound therapy markedly improves cognitive dysfunctions in mouse models of dementia—crucial roles of endothelial nitric oxide synthase,” *Brain Stimulat.*, vol. 11, no. 5, pp. 959–973, 2018.
- [56] T. Inubushi et al., “Effects of ultrasound on the proliferation and differentiation of cementoblast lineage cells,” *J. Periodontol.*, vol. 79, no. 10, pp. 1984–1990, 2008.
- [57] K. Bogovich, “Induction of ovarian cysts in progesterone-synchronized immature rats: Evidence that suppression of follicular aromatase activity is not a prerequisite for the induction of cystic follicles,” *Endocrinology*, vol. 124, no. 4, pp. 1646–1653, 1989.
- [58] K. Bogovich, “The impact of unabated stimulation by human chorionic gonadotropin on the steroid hormone environment of pregnant rats and the spontaneous expression of ovarian cysts in female progeny,” *Endocrine*, vol. 33, no. 2, pp. 152–164, Apr. 2008, doi: [10.1007/s12020-008-9072-z](https://doi.org/10.1007/s12020-008-9072-z).
- [59] N. Renier, Z. Wu, D. J. Simon, J. Yang, P. Ariel, and M. Tessier-Lavigne, “iDISCO: A simple, rapid method to immunolabel large tissue samples for volume imaging,” *Cell*, vol. 159, no. 4, pp. 896–910, 2014.